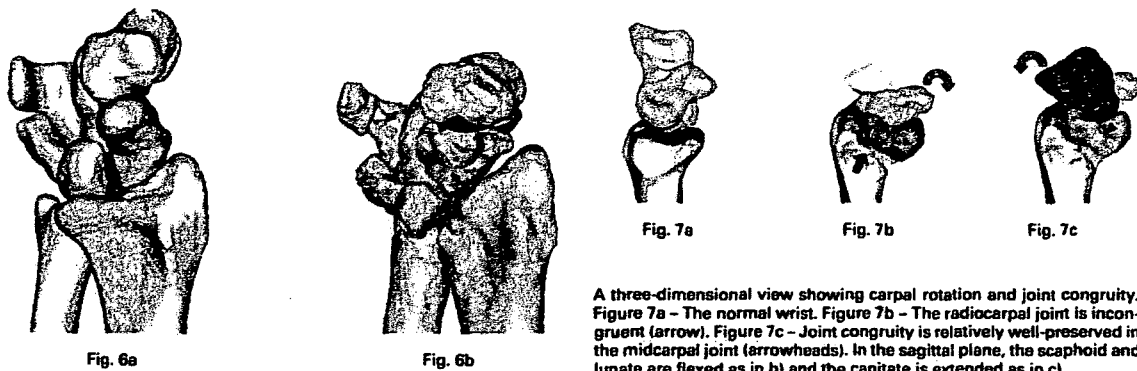


Diagrams showing centroid translocation from a) a dorsal view, b) ulnar view, c) distal view and d) radiopalmar view. All the centroids translocated in an ulnar, proximal and volar direction. The trapezium translated slightly in a dorsal direction according to the X component but, overall, translocated in a palmar direction (Tm, trapezium; Td, trapezoid; C, capitate; H, hamate; S, scaphoid; L, lunate; and T, triquetrum).



Three-dimensional radiopalmar view of the translation of the carpus in a) a normal wrist and b) rheumatoid arthritis. The carpus translocates along the direction of the slope of the joint surface of the distal radius.

palmar flexion with no significant rotation. Accurate estimation of carpal supination by plain radiography may not be easy since palmar subluxation of the distal radius in relation to the ulna makes it difficult to obtain a true lateral view for measurement of carpal rotation in the transverse plane.

We also noticed a different pattern of rotational deformity between the radiocarpal and midcarpal joints. Our 3D study showed that the proximal row as flexed at the radiocarpal joint and the distal row extended at the midcarpal joint (Fig. 7). While flexion of the proximal row was associated with translocation, the extension of the distal row was associated only with minor translocation. Although our patients had joint narrowing throughout the carpus, the congruity and function of the midcarpal joint were better preserved even in deformed RA wrists than at the radiocarpal joint.

Moritomo et al²⁰ proposed a self-stabilising mechanism which is stronger in the midcarpal than in the radiocarpal

joint. A scaphoid under axial load against the trapezium tends to rotate in a flexion/ulnar direction. This turning effect is constrained by the extension/radial deviation moment of the triquetrum, leading to a stable equilibrium provided that the interosseous ligaments in the proximal row are intact. We speculated that, with loosening of many carpal ligaments, the radiocarpal joint may easily lose congruity. Whereas the deformity in this joint included translational and rotational elements, in the midcarpal joint the deformity was predominantly rotational. We considered the radiocarpal joint to be more incongruent and thereby more prone to cartilaginous damage.

Our study has limitations, the most important of which is that it was based on selected cases in which the whole carpal bones were shifted to the ulnar side, but the shapes were relatively recognisable on plain radiography. The other limitation was that age and gender were not fully matched between the RA and control wrists. It is possible that calculation of centroids and angles of rotation are influenced by erosion of the carpal bones with a subsequent alteration of shape. Our quantitative information,

Table I. Details of translocation in the carpal bones

Direction	Centroid translocation																					
	Capitate			Hamate			Lunate			Scaphoid			Triquetrum			Trapezium			Trapezoid			
	AD* (mm)	TI†	SD	AD (mm)	TI	SD	AD (mm)	TI	SD	AD (mm)	TI	SD	AD (mm)	TI	SD	AD (mm)	TI	SD	AD (mm)	TI	SD	
Palmar																						
Normal	3.21	0.01	0.11	2.99	0.07	0.11	1.08	0.23	0.05	2.04	0.23	0.07	0.52	0.15	0.08	0.22	0.47	0.18	0.33	0.04	0.16	
RA‡		0.17	0.16		0.22	0.21		0.33	0.18		0.37	0.16		0.20	0.21		0.54	0.16		0.07	0.17	
Proximal																						
Normal	10.70	-0.57	0.14	9.41	-0.61	0.24	8.68	0.05	0.14	6.90	-0.20	0.06	9.89	-0.19	0.24	11.37	-0.83	0.16	13.30	-0.82	0.16	
RA		-0.15	0.20		-0.26	0.20		0.48	0.27		0.10	0.15		0.25	0.27		-0.42	0.16		-0.32	0.17	
Ulnar																						
Normal	6.28	0.19	0.19	4.68	0.70	0.19	5.07	0.35	0.09	7.10	-0.24	0.14	3.85	0.84	0.10	6.42	-0.49	0.26	6.12	-0.24	0.25	
RA		0.52	0.18		1.04	0.23		0.66	0.14		0.05	0.14		1.17	0.16		-0.27	0.18		0.00	0.17	


* AD, the absolute value of the difference of the mean translation (mm)

† TI, translocation index

‡ RA, rheumatoid arthritis

however, allowed early identification of the rheumatoid deformity and should be a guide to treatment, in particular in the decision as to whether to undertake radiocarpal fusion alone or to include the midcarpal joint.

Supplementary Material

 A further opinion by Dr Klemens Trieb is available with the electronic version of this article on our website at www.jbjs.org.uk

No benefits in any form have been received or will be received from a commercial party related directly or indirectly to the subject of this article.

References

- Shapiro JS. The wrist in rheumatoid arthritis. *Hand Clin* 1996;12:477-98
- Kusbeer DM, Braunstein EM, Buckwalter KA, Krohn K, White HA. Carpal instability in rheumatoid arthritis. *Can Assoc Radiol J* 1993;44:291-5.
- Muramatsu K, Ibara K, Tanaka H, Kawai S. Carpal instability in rheumatoid wrists. *Rheumatol Int* 2004;24:34-6.
- Shapiro JS. A new factor in the etiology of the ulnar drift. *Clin Orthop* 1970;68:32-43.
- Taleisnik J. Rheumatoid synovitis of the volar compartment of wrist joint: its radiological signs and its contribution to wrist and hand deformity. *J Hand Surg [Am]* 1979;4:526-35.
- Flury MP, Herren DB, Simmen BR. Rheumatoid arthritis of the wrist: classification related to the natural course. *Clin Orthop* 1999;366:72-7.
- Van Vught RM, van Jaarsveld CH, Hofman DM, Heiders PJ, Bijlman JW. Patterns of disease progression in the rheumatoid wrist: a long-term follow-up. *J Rheumatol* 1999;26:1467-73.
- Shapiro JS. Wrist involvement in rheumatoid arthritis swan-neck deformity. *J Hand Surg [Am]* 1982;7:484-91.
- Youm Y, McMurtry RV, Platt AE. Kinematics of the wrist: an experimental study of radial-ulnar deviation and flexion-extension. *J Bone Joint Surg [Am]* 1978;60-A:423-31.
- Ochi T, Iwase R, Kimura T, et al. Effect of early synovectomy on the course of rheumatoid arthritis. *J Rheumatol* 1991;18:1794-8.
- Lorenson WE, Cline HE. Marching cubes: a high resolution 3D surface construction algorithm. *Computer Graphics* 1987;21:163-9.
- Goto A, Moritomo H, Murase T, et al. In vivo three-dimensional wrist motion analysis using magnetic resonance imaging and volume-based registration. *J Orthop Res* 2005;23:750-6.
- Oka K, Moritomo H, Murase T, et al. Patterns of carpal deformity in scaphoid non-union: a 3-dimensional and quantitative analysis. *J Hand Surg [Am]* 2005;30:1136-44.
- Belsole RJ, Hibelink DR, Llewellyn JA, et al. Mathematical analysis of computed carpal models. *J Orthop Res* 1988;6:116-22.
- Belsole RJ, Hibelink DR, Llewellyn JA, Dale M, Ogden JA. Carpal orientation from computed reference axes. *J Hand Surg [Am]* 1991;16:82-90.
- Palmer AK. Fractures of the distal radius. In: Green DP, ed. *Operative hand surgery* Vol. 1. Third ed. New York: Churchill Livingstone, 1993:929-73.
- Scheibel FA, Linscheid RL, An KN, Chao EY. A normal data base of posteroanterior roentgenographic measurements of the wrist. *J Bone Joint Surg [Am]* 1992;74-A:1418-29.
- Cooney WP, Garcia-Elias M, Dobyns JH. Anatomy of mechanics of carpal instability. *Surg Rounds Orthop* 1989;3:15-24.
- Mizusaki T, Ikuta Y. The dorsal carpal ligament: their anatomy and function. *J Hand Surg [Br]* 1989;14:91-8.
- Moritomo H, Murase T, Goto A, et al. In vivo three-dimensional kinematics of the midcarpal joint of the wrist. *J Bone Joint Surg [Am]* 2006;88-A:611-21.

Long-Term Results of Surgery for Forearm Deformities in Patients with Multiple Cartilaginous Exostoses

By Shosuke Akita, MD, Tsuyoshi Murase, MD, Kazuo Yonenobu, MD, Kozo Shimada, MD, Kazuhiro Masada, MD, and Hideki Yoshikawa, MD, PhD

Investigation performed at the Department of Orthopaedic Surgery, Osaka University, and the Department of Orthopaedic Surgery, Osaka Minami Medical Center, Osaka, Japan

Background: Surgical treatment of forearm deformities in patients with multiple cartilaginous exostoses remains controversial. The purpose of the present study was to determine the reasonable indications for operative treatment and to evaluate long-term results of forearm surgery in these patients.

Methods: We retrospectively reviewed twenty-three patients (thirty-one forearms) after a mean duration of follow-up of nearly thirteen years. The mean age at the time of the initial procedure was eleven years. The patients underwent a variety of surgical procedures, including excision of exostoses; corrective procedures (lengthening of the radius or ulna and/or corrective osteotomy of the radius and/or ulna) and open reduction or excision of a dislocated radial head. Clinical evaluation involved the assessment of pain, activities of daily living, the cosmetic outcome, and the ranges of motion of the wrist, forearm, and elbow. The radiographic parameters that were assessed were ulnar variance, the radial articular angle, and carpal slip.

Results: Four patients had mild pain, and five patients had mild restriction of daily activities at the time of follow-up. Eight patients stated that the appearance of the forearm was unsatisfactory. Radiographic parameters (ulnar variance, radial articular angle, carpal slip) were initially improved; however, at the time of the final follow-up visit, the deformities had again progressed and showed no significant improvement. The only procedure that was associated with complications was ulnar lengthening. Complications included nonunion (three forearms), fracture of callus at the site of lengthening (two forearms), and temporary radial nerve paresis following an ulnar distraction osteotomy (one forearm). Excision of exostoses significantly improved the range of pronation ($p = 0.036$).

Conclusions: In our patients with multiple cartilaginous exostoses, corrective osteotomy and/or lengthening of forearm bones was not beneficial. The most beneficial procedure was excision of exostoses. Reasonable indications for forearm surgery in these patients are (1) to improve forearm rotation and (2) to improve the appearance.

Level of Evidence: Therapeutic Level IV. See Instructions to Authors for a complete description of levels of evidence.

Multiple cartilaginous exostoses, also known as multiple osteochondromata or diaphyseal aclasis, are characteristic of a disorder of endochondral bone growth that features abnormal metaphyseal bone prominences capped with cartilage, which are accompanied by de-

fective metaphyseal remodeling and asymmetrical retardation of longitudinal bone growth. Forearm deformities are seen in 30% to 60% of patients with multiple exostoses¹⁻⁴.

The most common deformities are a combination of relative shortening of the ulna, bowing of either or both fore-

Disclosure: The authors did not receive any outside funding or grants in support of their research for or preparation of this work. Neither they nor a member of their immediate families received payments or other benefits or a commitment or agreement to provide such benefits from a commercial entity. No commercial entity paid or directed, or agreed to pay or direct, any benefits to any research fund, foundation, division, center, clinical practice, or other charitable or nonprofit organization with which the authors, or a member of their immediate families, are affiliated or associated.

arm bones, increased ulnar tilt of the distal radial epiphysis, ulnar deviation of the hand, progressive ulnar translocation of the carpus, and dislocation of the head of the radius⁵⁻¹⁰. The treatment of forearm deformities in these patients is difficult because the long-term results have not been well documented, and there is a lack of consensus regarding the indications for surgery. The present study was performed because the long-term prognosis after operative intervention is uncertain. In addition, we attempted to define reasonable indications for the operative management of these patients.

Materials and Methods

Fifty patients were diagnosed as having multiple cartilaginous exostoses at Osaka University Hospital and Osaka Minami Medical Center between 1962 and 2000. In this group, thirty-four patients (forty-two forearms) had surgical treatment. We attempted to contact the patients who had already reached skeletal maturity (i.e., those who were at least eighteen years old). As a result, twenty-three patients (thirty-one forearms) were successfully contacted and evaluated at Osaka Minami Medical Center. These patients included seventeen men and six women who had a mean age of twenty-six years (range, eighteen to forty-eight years) at the time of evaluation. Eighteen of the twenty-three patients had a family history of the disease. Preoperative information was obtained from the medical records and radiographs. All of the subjects gave informed consent to participate in this study, which was approved by the institutional review board of Osaka Minami Medical Center.

Surgery

The operations on these patients involved three different types of procedures: excision of exostoses, corrective procedures, and excision or open reduction of the dislocated head of the radius. Excision of exostoses was the primary procedure in all cases. The corrective procedures included lengthening or corrective osteotomy of the ulna or radius.

The twenty-three patients (thirty-one forearms) underwent a variety of procedures, either alone or in combination, including (1) excision of exostoses (thirty-one forearms), (2) lengthening of the ulna (sixteen forearms), (3) lengthening of the radius (four forearms), (4) corrective osteotomy of the radius (fourteen forearms), (5) corrective osteotomy of the ulna (two forearms), (6) open reduction of the dislocated radial head (two forearms), and (7) excision of the radial head (two forearms). In both patients who underwent open radial head reduction, we simultaneously performed an immediate ulnar lengthening, a corrective osteotomy of the radius, and anular ligament reconstruction with palmaris longus tendon graft.

Seven of the thirty-one forearms underwent more than one operation. Nineteen of the twenty-three patients underwent surgery before reaching skeletal maturity; the mean age at the time of the initial procedure was eleven years (range, three to twenty-three years). The mean follow-up interval between the final surgical procedure and the time of evaluation was 12.8 years (range, six to thirty-nine years) (see Appendix).

Surgical Indications

Exostoses were removed if (1) there was interference with joint movement or if (2) the lesion was prominent, painful, and/or cosmetically undesirable.

The indications for performing corrective procedures were (1) a discrepancy of >5 mm between the lengths of the ulna and radius with or without bowing, (2) a radial articular angle of >30°, (3) a carpal slip of >60%, (4) bowing of the radius, or (5) a combination of these changes. Most patients had a combination of these changes.

Symptomatic dislocation of the head of the radius was defined as interfering with joint movement or causing pain.

Clinical Evaluation

An experienced hand surgeon (S.A.) who had not been involved in the surgical procedures interviewed the patients with use of a questionnaire that evaluated the outcome with respect to pain, activities of daily living, and the appearance of the forearm. Pain and restriction of activities were classified into four categories (none, mild, moderate, or severe), whereas the appearance of the forearm was classified as satisfactory or unsatisfactory. The evaluation form can be found in the Appendix. In addition, the ranges of motion of the wrist, forearm, and elbow were measured, and the grip strength was also determined.

Radiographic Evaluation

We examined radiographs of both wrists, forearms, and elbows for each subject. The forearms were classified into three morphological types according to the system of Masada et al.¹¹ In type-I forearms, the main exostosis arises from the distal part of the ulna. The ulna is relatively short and there is bowing of the radius, but the radial head is not dislocated. Both tapering of the ulnar head and ulnar tilt of the distal part of the radius are observed. In type-II forearms, there is ulnar shortening along with dislocation of the radial head, but bowing of the radius is less severe than in type-I forearms because of the dislocation. Type-II forearms are separated into two subgroups. In type-IIa forearms, dislocation of the radial head is caused by an exostosis arising from the proximal part of the radius, whereas in type-IIb forearms the dislocation is not due to such an exostosis. In type-III forearms, the main exostosis arises from the distal part of the radius and there is a relative shortening of the radius.

Ulnar variance, the radial articular angle, and carpal slip were also measured. The radial articular angle and carpal slip were measured with use of the system of Fogel et al.⁵ The radial articular angle was defined as the angle between a line running along the articular surface of the radius and another line that was perpendicular to a line joining the center of the radial head to the radial border of the distal radial epiphysis (the radial styloid in skeletally mature subjects) (Fig. 1). The normal range of this angle was 15° to 30°^{5,11}. Carpal slip was measured by determining the percentage of the lunate that was in contact with the radius. First, a line was drawn from the center of the olecranon through the ulnar border of the radial

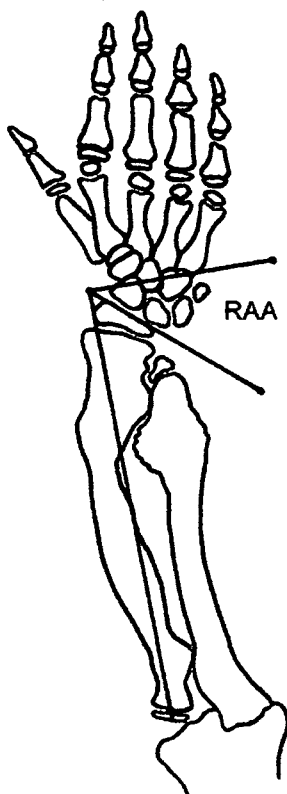


Fig. 1

The radial articular angle (RAA) was defined as the angle between a line running along the articular surface of the radius and another line that was perpendicular to a line joining the center of the radial head to the radial border of the distal radial epiphysis (the radial styloid in skeletally mature subjects). The normal range of this angle is 15° to 30° ^{5,11}.

epiphysis (the radial articular surface in skeletally mature subjects) (Fig. 2). This line normally bisects the lunate. An abnormal carpal slip was defined as being present when ulnar displacement of the lunate exceeded 50%^{5,11}.

Radiographs were also examined for degenerative changes of the joints, which were defined as narrowing of the joint space and/or the formation of osteophytes. Deformity of the radial head was considered to be present if there was evidence of hypertrophy or flattening.

Statistical Analysis

A paired two-group t test was used for comparing data from pairs of groups, and the Mann-Whitney U test was used for data from unpaired groups. The level of significance was set at $p < 0.05$.

Results

Clinical Outcome

Four patients (four upper extremities) complained of mild pain when performing strenuous activities, whereas the other nineteen patients (twenty-seven upper extremities) had

no pain at the time of follow-up. Five patients (five forearms) noted mild restriction of daily activities, but the other eighteen patients (twenty-six forearms) stated that they had no restrictions. These five patients generally showed limitation of either pronation or supination, or both, but their daily activities were minimally affected. Eight patients (eight forearms) stated that the appearance of the forearm was unsatisfactory, and this unsatisfactory appearance was of greater importance to these patients than any pain or restriction of activities.

At the time of the final follow-up evaluation, the mean wrist flexion (and standard deviation) was $59^{\circ} \pm 16^{\circ}$, the mean extension was $66^{\circ} \pm 9^{\circ}$, the mean radial deviation was $14^{\circ} \pm 13^{\circ}$, and the mean ulnar deviation was $43^{\circ} \pm 10^{\circ}$. The mean forearm pronation was $65^{\circ} \pm 27^{\circ}$, and the mean supination was $73^{\circ} \pm 23^{\circ}$. The mean elbow flexion was $138^{\circ} \pm 11^{\circ}$, and the mean lack of extension was $2^{\circ} \pm 10^{\circ}$. The mean range of motion at the time of the final follow-up was not significantly improved compared with the preoperative range, except for a significant increase of forearm pronation from 43° to 65° ($p = 0.004$). The average grip strength was 25.0 kg (Table I).

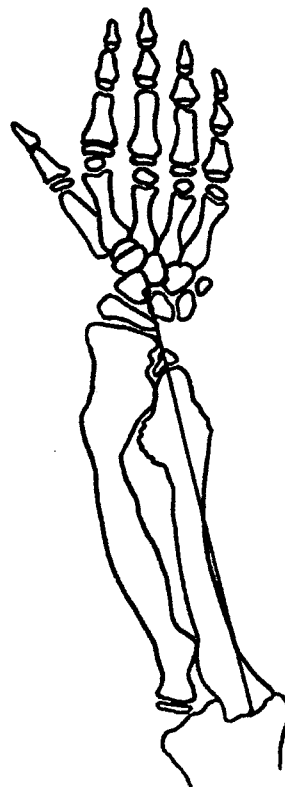


Fig. 2

Carpal slip was measured by determining the percentage of the lunate that was in contact with the radius. First, a line was drawn from the center of the olecranon through the ulnar border of the radial epiphysis (the radial articular surface in skeletally mature subjects). This line normally bisects the lunate. An abnormal carpal slip was defined as being present when ulnar displacement of the lunate exceeded 50%^{5,11}.

TABLE I Range of Movement and Grip Power

Function	Mean Value (Range)		P Value†
	Preoperative	Postoperative	
Wrist			
Flexion (deg)	65 (30 to 90)	59 (25 to 80)	NS
Extension (deg)	68 (25 to 85)	66 (45 to 80)	NS
Radial deviation (deg)	14 (-15 to 45)	14 (-15 to 50)	NS
Ulnar deviation (deg)	36 (10 to 60)	43 (20 to 60)	NS
Forearm			
Pronation (deg)	43 (0 to 90)	65 (0 to 90)	0.004
Supination (deg)	61 (-30 to 100)	73 (0 to 100)	NS
Elbow			
Flexion (deg)	132 (95 to 150)	138 (95 to 150)	NS
Extension (deg)	-3 (-30 to 10)	-2 (-35 to 15)	NS
Grip power (kg)	NA*	25.0 (10 to 40)	

*NA = preoperative data were not available. †Paired two-group t test. NS = not significant.

Radiographic Outcome

According to the system of Masada et al., twenty-one forearms were classified as type I, five were classified as type II (with two being classified as type IIa and three being classified as type IIb), and five were classified as type III. Preoperative radiographs were available for thirty of the thirty-one forearms. The average preoperative ulnar variance and radial articular angle for these thirty forearms were -6.0 mm and 40°, respectively, whereas the average preoperative carpal slip in twenty-seven forearms was 53% (the lunate was not ossified in three of the thirty forearms). At the time of the most recent follow-up of all thirty-one forearms, the average ulnar variance, radial articular angle, and carpal slip were -3.5 mm, 41°, and 43%, respectively. When all of the patients were compared, there was no significant improvement in any of these three parameters (Table II). These parameters were not related to the range of motion of the upper extremity, but each radiographic parameter was related to the cosmetic outcome ($p = 0.0129$, $p = 0.0003$, and $p = 0.0155$ for ulnar variance, the radial articular angle, and

carpal slip, respectively; Mann-Whitney U test).

Of the thirty-one extremities, two showed degenerative changes of the elbow joint at the time of follow-up; the changes were osteophytes in both cases. These two forearms had a type-II deformity, and there was mild restriction of daily activities due to limited elbow range of motion. No evidence of degenerative changes was seen at the wrist joint in any of the patients.

With the exclusion of the two limbs that were treated by radial head resection, there was radial head deformity in ten (34%) of twenty-nine extremities. Radial head deformity was unrelated to degenerative changes of the elbow joint and did not influence the range of motion of the upper extremity.

Outcome of Corrective Procedures

Lengthening and/or corrective osteotomy of the radius or ulna was done alone or in combination in eighteen forearms. The average preoperative ulnar variance, radial articular angle, and carpal slip were -8.3 mm, 42°, and 62%, respectively. In six of these forearms, further progression of deformity necessitated

TABLE II Radiographic Parameters

Radiographic Parameters	Mean Value (Range)		P Value*
	Preoperative	Postoperative	
Ulnar variance (mm)	-6.0 (-29 to 10)	-3.5 (-17 to 7)	NS
Radial articular angle (deg)	40 (20 to 80)	41 (27 to 60)	NS
Carpal slip (%)	53 (0 to 100)	43 (13 to 64)	NS

*Paired two-group t test. NS = not significant.

revision surgery. Almost all of these forearms had severe deformity, and as many as four corrective operations were performed. At one year after the final corrective procedure, the measured parameters averaged -1.5 mm, 38° , and 40% , respectively, and there was significant improvement in ulnar variance ($p = 0.005$) and carpal slip ($p = 0.01$). Although forearm deformities initially demonstrated improvement, we found subsequent progression over the long term after the corrective surgery. At the time of the most recent follow-up, ulnar variance averaged -4.0 mm, the radial articular angle averaged 44° , and carpal slip averaged 44% . When we assessed the effect of the corrective procedures, radiographic parameters also demonstrated initial improvement; however, the deformities had progressed by the time of the most recent follow-up visit, and there was no significant improvement over the long term.

The only corrective procedure that was associated with complications was ulnar lengthening. A total of eighteen ulnar lengthening procedures were performed in sixteen forearms. In eight cases the lengthening was performed gradually with use of external distraction, whereas in ten cases it was done immediately with the insertion of a bone graft or the performance of a step-cut osteotomy. Complications included nonunion in three forearms, fracture of callus at the site of lengthening in two forearms, and temporary radial nerve paresis (paresthesia in the radial nerve territory and weakness of finger extensors) in one forearm. One of the three nonunions occurred after an immediate ulnar lengthening. The other two nonunions occurred in one patient who was managed with gradual bilateral ulnar lengthening after reaching skeletal maturity; this patient also had radial nerve paresis, as mentioned above. In the three forearms with nonunion, osseous union was eventually achieved uneventfully by means of bone-grafting and internal fixation. Fracture of a callus was treated with plaster cast immobilization in one patient and with intramedullary fixation in the other patient. The patient with radial nerve dysfunction during distraction of the ulna showed distal migration of the radius. This migration was easily reduced by dividing the cord-like portion of the interosseous membrane, and the radial nerve dysfunction resolved completely.

Outcome of Excision of Exostoses

Excision of exostoses was performed in all of the patients. Ten patients (eleven forearms) were managed only with excision procedures. The mean age of these ten patients was 11.2 years (range, five to sixteen years). The location of the excised exostoses was the distal part of the radius in eight forearms, the distal part of the ulna in two forearms, and both the distal part of the radius and the distal part of the ulna in one forearm. Simple excision of exostoses significantly improved the range of pronation ($p = 0.036$). With the numbers available, there were no significant differences between locations with regard to improvement in forearm rotation. In these eleven forearms, the preoperative ulnar variance, radial articular angle, and carpal slip averaged -2.0

mm, 35° , and 37% , respectively. At the time of follow-up, these three parameters averaged -3.6 mm, 40° , and 42% , respectively, and there was no significant change in any of the three parameters. There were no complications of simple excision, and the ten patients who underwent simple excision procedures had no symptoms at the time of the most recent follow-up.

Outcome of Radial Head Surgery

Dislocation of the head of the radius (a type-II deformity) was observed in five extremities. Along with open reduction of the dislocated radial head, we performed immediate ulnar lengthening, corrective osteotomy of the radius, and anular ligament reconstruction with palmaris longus tendon graft in two patients (two forearms) before they reached skeletal maturity, but these procedures were not effective in either case. Both patients had evidence of degenerative changes at the elbow joint as well as restricted motion of the elbow and restricted pronation of the forearm at the time of the most recent follow-up.

Excision of the dislocated radial head was performed in two patients (two forearms) after skeletal maturity. Both patients had pain and restricted motion of the forearm before surgery. In both patients, pain was relieved and the range of motion of the forearm was improved at the time of the most recent follow-up.

Discussion

The present study assessed the long-term results of surgical treatment of forearm deformities in patients with multiple cartilaginous exostoses in an attempt to determine the reasonable indications for such surgery. On the basis of our findings, surgery in these patients is indicated for two purposes: (1) to improve forearm pronation when it is restricted by an exostosis (with the most effective procedure being simple excision of the exostosis) and (2) to improve the appearance of the forearm.

The present study had several weaknesses. It was a retrospective case review without any controls (nonoperatively treated extremities), only twenty-three of thirty-four patients were available for the final follow-up evaluation, and some preoperative data (grip strength) were unavailable. Furthermore, a variety of operative procedures were performed (often in combination), making it difficult to draw definite conclusions. However, little information has been published on the functional outcome for patients with multiple cartilaginous exostoses who have undergone corrective forearm surgery, and, to our knowledge, there have been no previous reports about the long-term results of surgical treatment of forearm deformities. Therefore, our data may be useful for selecting among treatment options.

A number of techniques for the surgical treatment of forearm deformities have been described^{5,7,9,11-15}, but the operative treatment of such deformities in patients with multiple cartilaginous exostoses remains controversial^{14,15}. Fogel et al. concluded that deformities of the forearm should be treated

early and aggressively to prevent disability by employing procedures such as excision of exostoses and ulnar lengthening with or without radial hemiepiphysal stapling or osteotomy⁵. Peterson reported that forearm deformities were the most frequent cause of functional impairment in patients with multiple exostoses and advocated aggressive management as soon as it became clear that the growth of the affected bones was being altered, stating that prevention of progressive deformity and functional impairment were the paramount goals⁶. However, Stanton and Hansen evaluated the radiographic anatomy, functional outcome, and impairment ratings of twenty-eight patients with hereditary multiple exostoses and concluded that reasonable function was preserved despite the occurrence of deformity¹⁶. Arms et al. performed a telephone questionnaire evaluation of thirty-seven patients who had forearm deformities and found that most patients maintained adequate function after reaching skeletal maturity despite having severe deformity¹⁷. Likewise, we found that there was little restriction of daily activities in patients with a residual forearm deformity postoperatively and that radiographic parameters were not related to the final range of motion of the upper extremity.

Noonan et al. assessed the functional outcome for the forearm in a study of thirty-nine adults (seventy-seven forearms) with a mean age of forty-two years who had multiple hereditary osteochondromatosis and had not undergone corrective surgery¹⁴. Although we cannot fully compare those results with the postoperative functional results in our series, a review of their results for untreated patients suggests that corrective surgery did not achieve any marked improvement in function. They also reported that the appearance of the forearm was not related to the functional outcome. Likewise, our findings indicate that most forearm deformities do not influence the functional outcome. However, we found that postoperative radiographic parameters were related to complaints about the appearance of the upper extremity. Noonan et al. reported that seventeen (44%) of thirty-nine patients found the arms to be cosmetically unappealing because of shortening, angulation, or bumps¹⁴. Wood et al., in a report on ten patients who had undergone various operations (including corrective procedures such as forearm bone lengthening and/or osteotomy), concluded that, although function only showed minimal improvement, the appearance of the limbs was markedly improved⁹. Pritchett, in a report on the results of ulnar lengthening in eight patients (ten forearms), concluded that there was improvement in the appearance, forearm movement, and radial head stability⁷. Therefore, when the patient finds the appearance of the forearm to be problematic, corrective surgery may be a reasonable option. However, Pritchett also reported that partial recurrence of forearm deformities occurred in skeletally immature patients⁷, and we similarly found that deformity sometimes progressed after corrective surgery. The reported complication rate for lengthening of the forearm has varied widely, from 0% to 100%^{5,7,11,18}. In the present series, complications occurred in association with five (28%) of eighteen ulnar length-

ening procedures, suggesting that this operation should be performed with great caution.


Previously, we believed that forearm deformities were the most frequent cause of functional impairment, and we recommended corrective procedures to prevent progressive deformity and functional impairment. Our surgical indications included a discrepancy of >5 mm between the lengths of the ulna and radius with or without bowing, a radial articular angle of >30°, a carpal slip of >60%, bowing of the radius, or a combination of these changes. However, we now think that forearm deformities are unrelated to function and we no longer recommend corrective procedures for the prevention of functional impairment.

Fogel et al. reported that the excision of exostoses could not correct deformities but might arrest or retard their progression⁵. Shin et al. reported that the simple excision of exostoses did not improve the radiographic parameters but led to a significant increase in supination of the forearm ($p = 0.049$)¹⁹. We also found that excision of exostoses alone did not correct forearm deformities, but simple excision achieved significant improvement of forearm pronation and might also retard the progression of deformities.

Stanton and Hansen reported that the status of the radial head was not associated with either the subjective assessment score or with the level of performance in the hand test of Jebsen¹⁶. In addition, Dahl stated that he did not perform direct reduction of a chronically dislocated radial head because stiffness and pain could occur²⁰. In the present series, dislocation of the radial head was treated with open reduction (two forearms), excision (two forearms), and observation (one forearm). Radial head reduction was not effective in either patient, with degenerative changes of the elbow joint and restricted movement of both the elbow and forearm (causing slight limitation of daily activities) being evident at the time of the most recent follow-up. Excision of the dislocated radial head and observation were both associated with a better outcome as there was no degeneration of the elbow joint and a good range of motion of the upper extremity was maintained. However, because the numbers were small in this series, it is difficult to draw firm conclusions.

In summary, we believe that simple exostosis excision is reasonable when there is restriction of forearm pronation. When the primary concern is appearance, a corrective procedure is an option; however, it should be viewed with caution as there can be recurrence of deformity, especially in immature patients, and nonunion may occur following ulnar lengthening. As an alternative, simple exostosis excision may retard the progression of forearm deformity.

Appendix

 Tables showing the details on all study subjects and the questionnaire used in this study are available with the electronic versions of this article, on our web site at jbjs.org (go to the article citation and click on "Supplementary Material") and on our quarterly CD-ROM (call our subscription department, at 781-449-9780, to order the CD-ROM). ■

Shosuke Akita, MD
Kazuo Yonenobu, MD
Department of Orthopaedic Surgery, National Hospital Organization
Osaka Minami Medical Center, 2-1 Kidohigashi, Kawachinagano, Osaka
586-8521, Japan. E-mail address for S. Akita: akita@eos.ocn.ne.jp

Tsuyoshi Murase, MD
Hideki Yoshikawa, MD, PhD
Department of Orthopaedic Surgery, Osaka University Graduate School

of Medicine, 2-2 Yamadaoka, Suita 565-0871, Japan

Kozo Shimada, MD
Department of Orthopaedic Surgery, Rinku General Medical Center, 2-
23 Rinku Orai-kita, Izumisano, Osaka 598-8577, Japan

Kazuhiro Masada, MD
Masada Orthopaedic Rheumatology Clinic, 779-2 Nagasone, Sakai, Os-
aka 591-8025, Japan

References

1. Jaffe HL. Hereditary multiple exostosis. *Arch Pathol.* 1943;36:335-57.
2. Solomon L. Bone growth in diaphyseal aclasis. *J Bone Joint Surg Br.* 1961; 43:700-16.
3. Shapiro F, Simon S, Glimcher MJ. Hereditary multiple exostoses. Anthropometric, roentgenographic, and clinical aspects. *J Bone Joint Surg Am.* 1979; 61:815-24.
4. Schmale GA, Conrad EU 3rd, Raskind WH. The natural history of hereditary multiple exostoses. *J Bone Joint Surg Am.* 1994;76:986-92.
5. Fogel GR, McElfresh EC, Peterson HA, Wicklund PT. Management of deformities of the forearm in multiple hereditary osteochondromas. *J Bone Joint Surg Am.* 1984;66:670-80.
6. Peterson HA. Deformities and problems of the forearm in children with multiple hereditary osteochondromata. *J Pediatr Orthop.* 1994;14:92-100.
7. Pritchett JW. Lengthening the ulna in patients with hereditary multiple exostoses. *J Bone Joint Surg Br.* 1986;68:561-5.
8. Solomon L. Hereditary multiple exostosis. *J Bone Joint Surg Br.* 1963;45: 292-304.
9. Wood VE, Sauser D, Mudge D. The treatment of hereditary multiple exostosis of the upper extremity. *J Hand Surg [Am].* 1985;10:505-13.
10. Burgess RC, Cates H. Deformities of the forearm in patients who have multiple cartilaginous exostosis. *J Bone Joint Surg Am.* 1993;75:13-8.
11. Masada K, Tsuyuguchi Y, Kawai H, Kawabata H, Noguchi K, Ono K. Operations for forearm deformity caused by multiple osteochondromas. *J Bone Joint Surg Br.* 1989;71:24-9.
12. Rodgers WB, Hall JE. One-bone forearm as a salvage procedure for recalcitrant forearm deformity in hereditary multiple exostoses. *J Pediatr Orthop.* 1993;13:587-91.
13. Siffert RS, Levy RN. Correction of wrist deformity in diaphyseal aclasis by stapling. Report of a case. *J Bone Joint Surg Am.* 1965;47:1378-80.
14. Noonan KJ, Levenda A, Snead J, Feinberg JR, Mih A. Evaluation of the forearm in untreated adult subjects with multiple hereditary osteochondromatosis. *J Bone Joint Surg Am.* 2002;84:397-403.
15. Ip D, Li YH, Chow W, Leong JC. Reconstruction of forearm deformities in multiple cartilaginous exostoses. *J Pediatr Orthop B.* 2003;12:17-21.
16. Stanton RP, Hansen MO. Function of the upper extremities in hereditary multiple exostoses. *J Bone Joint Surg Am.* 1996;78:568-73.
17. Arms DM, Strecker WB, Manske PR, Schoenecker PL. Management of forearm deformity in multiple hereditary osteochondromatosis. *J Pediatr Orthop.* 1997;17:450-4.
18. Waters PM, Van Heest AE, Emans J. Acute forearm lengthenings. *J Pediatr Orthop.* 1997;17:444-9.
19. Shin EK, Jones NF, Lawrence JF. Treatment of multiple hereditary osteochondromas of the forearm in children: a study of surgical procedures. *J Bone Joint Surg Br.* 2006;88:255-60.
20. Dahl MT. The gradual correction of forearm deformities in multiple hereditary exostoses. *Hand Clin.* 1993;9:707-18.

The in Vivo Isometric Point of the Lateral Ligament of the Elbow

By Hisao Moritomo, MD, PhD, Tsuyoshi Murase, MD, PhD, Sayuri Arimitsu, MD, Kunihiro Oka, MD, Hideki Yoshikawa, MD, PhD, and Kazuomi Sugamoto, MD, PhD

Investigation performed at the Department of Orthopaedics, Osaka University Graduate School of Medicine, Osaka, Japan

Background: Many reports have discussed reconstruction of the lateral ulnar collateral ligament for the treatment of posterolateral rotatory instability of the elbow, but information regarding the isometric point of the lateral ligament of the elbow is limited. The purposes of the present study were to investigate the in vivo and three-dimensional length changes of the lateral ulnar collateral ligament and the radial collateral ligament during elbow flexion in order to clarify the role of these ligaments as well as to identify the isometric point for the reconstructed lateral ulnar collateral ligament on the humerus where the grafted tendon should be anchored.

Methods: We studied in vivo and three-dimensional kinematics of the normal elbow joint with use of a markerless bone-registration technique. Magnetic resonance images of the right elbows of seven healthy volunteers were acquired in six positions between 0° and 135° of flexion. We created three-dimensional models of the elbow bones, the lateral ulnar collateral ligament, and the radial collateral ligament. The ligament models were based on the shortest calculated paths between each origin and insertion in three-dimensional space with the bone as obstacles. We calculated two types of three-dimensional distances for the ligament paths with each flexion position: (1) between the center of the capitellum and the distal insertions of the ligaments (to investigate the physiological change in ligament length) and (2) between eight different humeral origins and the one typical insertion of the lateral ulnar collateral ligament (to identify the isometric point of the reconstructed lateral ulnar collateral ligament).

Results: The three-dimensional distance for the lateral ulnar collateral ligament was found to increase during elbow flexion, whereas that for the radial collateral ligament changed little. The path of the lateral ulnar collateral ligament gradually developed a detour because of the osseous protrusion of the lateral condyle with flexion. The most isometric point for the reconstructed lateral ulnar collateral ligament was calculated to be at a point 2 mm proximal to the center of the capitellum.

Conclusions: The radial collateral ligament is essentially isometric, but the lateral ulnar collateral ligament is not. The lateral ulnar collateral ligament is loose in elbow extension and becomes tight with elbow flexion.

Clinical Relevance: The present study suggests that the isometric point for the lateral ulnar collateral ligament graft origin is approximately 2 mm proximal to the center of the capitellum.

The function of the lateral ligament of the elbow has been primarily investigated by the application of tensile forces with valgus, varus, or rotational stresses applied to the dissected ligament¹⁻³. The current paradigm that deals with the change of length of the lateral ligament depends almost exclusively on the classic paper by Morrey and An,

which was published in 1985⁴. Those authors investigated the three-dimensional distance between the origin and insertion of the lateral collateral ligament complex and reported that the length of the lateral collateral ligament changed little during elbow flexion. This finding was consistent with the observation that the axis of rotation of the elbow passes through the

Disclosure: In support of their research for or preparation of this work, one or more of the authors received, in any one year, outside funding or grants of less than \$10,000 from Grants-in-Aid for Scientific Research, the Ministry of Education, Science and Culture of Japan. Neither they nor a member of their immediate families received payments or other benefits or a commitment or agreement to provide such benefits from a commercial entity. No commercial entity paid or directed, or agreed to pay or direct, any benefits to any research fund, foundation, division, center, clinical practice, or other charitable or nonprofit organization with which the authors, or a member of their immediate families, are affiliated or associated.

center of the capitellum^{4,6}. However, in that study, Morrey and An did not distinguish the lateral ulnar collateral ligament from the lateral collateral ligament complex. To our knowledge, there have been no reports of studies specifically dealing with the change in length of the lateral ulnar collateral ligament.

Furthermore, all of the current information dealing with the function of the elbow ligaments has been acquired in cadaver studies involving invasive procedures. Such *in vitro* experiments cannot completely reproduce the muscular force that is exerted across the elbow *in vivo*. This limitation could alter the normal *in vivo* kinematics of the ligaments. Recently, researchers have been able to measure *in vivo* kinematics of the human joint with use of a noninvasive technique^{7,9}, and Marai et al. reported a novel method for calculating ligament length noninvasively in three-dimensional space with bone obstacles (osseous protrusions that deflect a ligament path by ligament-bone impingement)¹⁰.

Posterolateral rotatory instability following disruption of the lateral collateral ligament is the most common form of recurrent posttraumatic instability of the elbow¹¹. It has been theorized that disruption of the lateral ulnar collateral ligament has a crucial role in the development of posterolateral rotatory instability^{11,12}. However, some biomechanical studies

have cast doubt on this theory¹³. Dunning et al., in a study of sequential sectioning of the lateral ulnar elbow ligament, reported that, compared with the intact elbow, no differences in the magnitude of laxity of the ulna were detected with only the radial collateral ligament intact³. Many reports dealing with lateral ulnar collateral ligament reconstruction for the treatment of posterolateral rotatory instability of the elbow have been published¹³⁻¹⁵. In addition, information is limited regarding the *in vivo* isometric point of the lateral ulnar collateral ligament of the elbow. The purposes of the present study were to investigate the *in vivo* and three-dimensional length changes of the lateral ulnar collateral ligament and the radial collateral ligament during elbow flexion in order to clarify the role of these ligaments as well as to identify the isometric point for the reconstructed lateral ulnar collateral ligament on the humerus where the grafted tendon should be anchored.

Materials and Methods

We studied the right elbow joints of seven healthy volunteers during elbow flexion with use of a noninvasive, *in vivo*, three-dimensional motion-analysis system. The patients included five men and two women with a mean age of 28.3 years (range, twenty-four to thirty-three years). All patients consented to be included in the study. The steps in this analysis

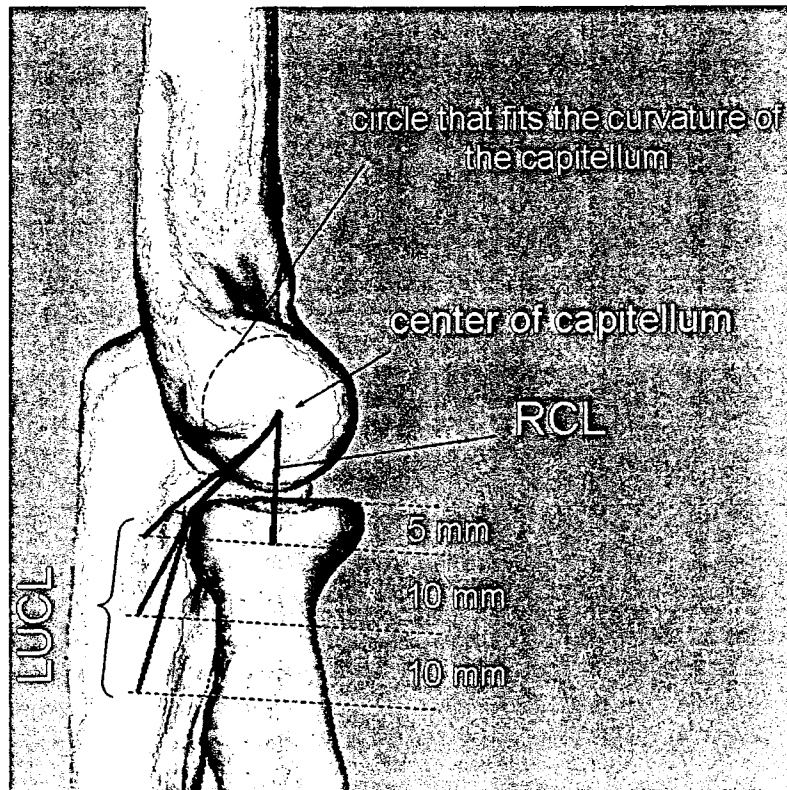


Fig. 1

The paths of the lateral ulnar collateral ligament (LUCL) and the radial collateral ligament (RCL) of the right elbow of a representative case.

included image acquisition, segmentation, and registration. A mathematical description of the motion of the individual bones and their relative motion was derived by computing the rigid transformation required to match the volume data of the models.

Magnetic resonance images of the right elbow of each volunteer were acquired in six positions of elbow flexion (0° , 30° , 60° , 90° , 120° , and 135°) with the same method as was used in our previous study⁷. During this elbow flexion study, the forearm was fixed in the neutral position. Regions of individual bones were semi-automatically segmented from magnetic resonance volume images with use of a software program (Virtual Place-M; AZE, Tokyo, Japan). The software generated three-dimensional surface bone models with use of the marching cubes technique¹⁶. Volume-based registration was done to determine relative positions between volume images represented at different coordinates⁹. Visualization of the geometrical models of each elbow was obtained with a software program that was developed in our laboratory (Orthopedics Viewer; Osaka University, Osaka, Japan).

Ligament Paths

We created three-dimensional models of the ligament paths that approximated the lateral ulnar collateral ligament and the radial collateral ligament. The ligament models were calculated as the shortest paths in three-dimensional space with bone obstacles on the basis of the method proposed by Marai et al.¹⁰. In this program, the paths can be detoured by osseous protrusions to avoid bone penetration. The structural and material properties of the ligaments are not taken into account in this program.

The origins and insertions of the ligament models that are reported in the present study were based solely on the osseous geometry of the elbow. We used anatomical landmarks to identify the origin and insertion points of the ligaments on the bone surfaces.

Normal Length Changes of the Ligaments

We created the ligament paths between the center of the capitel-

lum and the distal insertions of the lateral ulnar collateral ligament and the radial collateral ligament to investigate the normal length changes of the ligaments. In the present study, the origins of both the lateral ulnar collateral ligament and the radial collateral ligament were located at the center of the capitellum⁴, which was determined as the center of a circle that fit the curvature of the capitellum on the lateral view (Fig. 1). The insertion of the radial collateral ligament was placed at the most lateral point of the radial head at a level 5 mm distal to the proximal surface of the radial head. A previous anatomic study demonstrated that the lateral ulnar collateral ligament and the annular ligament form a broad conjoint insertion measuring approximately 2 cm in width¹⁷. On the basis of that study, three insertion points of the lateral ulnar collateral ligament, located 5, 15, and 25 mm distal to the proximal margin of the radial head, were placed on the supinator crest of the ulna. We calculated the three-dimensional distances of the paths of the lateral ulnar collateral ligament and radial collateral ligament between the origin and insertion of each ligament in six positions of flexion (0° , 30° , 60° , 90° , 120° , and 135°).

Length Changes of the Reconstructed Lateral Ulnar Collateral Ligament

Our goal was to find the isometric point of the reconstructed lateral ulnar collateral ligament at which the ligament's length change would be minimized during elbow flexion. We calculated the length changes of eight possible ligament paths of the reconstructed lateral ulnar collateral ligament on the basis of the eight different humeral origins other than the center of the capitellum and the one typical insertion of the lateral ulnar collateral ligament. The eight different possible origins were defined on the basis of their proximal and anterior locations from the center of the capitellum (Fig. 2, A) and were located at 2-mm intervals. These origins were located on the intersection of a grid whose lines were parallel or perpendicular to the longitudinal axis of the humerus. We first calculated the length changes of each possible ligament path between 0° and 135° of flexion (Figs. 2, B and 2, C) and determined the most isometric point of the reconstructed lateral ulnar collateral lig-

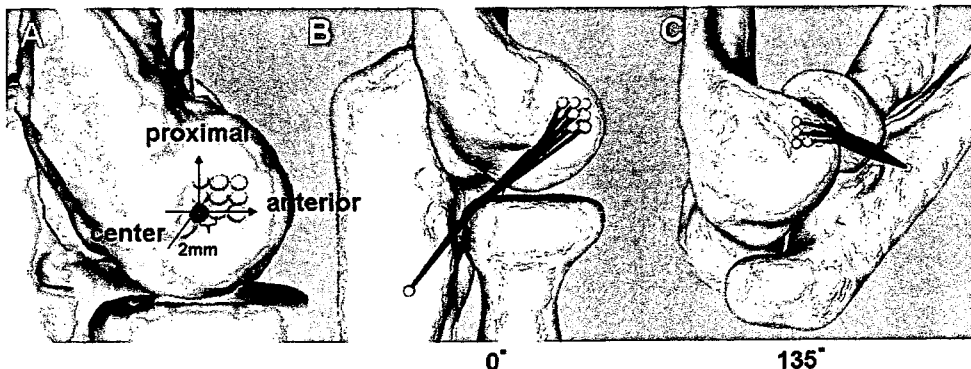


Fig. 2

A: The nine humeral origins of the reconstructed lateral ulnar collateral ligament, separated by 2-mm intervals on the capitellum. B and C: The ligament paths at 0° (B) and 135° of flexion (C) in a representative case.

TABLE I Data on the Ligament Length for Each of the Seven Elbows*

Case	Age (yr)	Gender	Length Change of Normal Ligaments from 0° to 135° of Flexion† (mm)			
			RCL	LUCL-1	LUCL-2	LUCL-3
1	30	M	1.6	2.8	3.0	2.6
2	33	M	1.1	4.0	3.4	2.4
3	25	M	-0.5	4.3	2.2	1.5
4	24	M	0.3	4.0	2.7	2.0
5	25	F	-1.3	2.9	2.5	2.0
6	30	F	0.8	2.8	1.9	1.3
7	31	M	0.1	3.7	2.0	1.2
Average	28.3		0.3	3.5	2.5	1.9
Standard Deviation			1.0	0.7	0.5	0.5

*RCL = radial collateral ligament, and LUCL = lateral ulnar collateral ligament. †The ulnar insertion points of LUCL-1, 2, and 3 are 5, 15, and 25 mm distal to the radial head, respectively. ‡The first value for each humeral origin indicates the anterior distance from the humeral origin to the center of the capitellum, and the second value indicates the proximal distance from the humeral origin to the center of the capitellum.

ament at which the ligament's length change was the smallest. Then, at six flexion positions (0°, 30°, 60°, 90°, 120°, and 135°), we calculated the length change of the reconstructed ligament that had its origin at the isometric point. We defined the insertion point on the ulna to be 15 mm distal from the proximal margin of the radial head.

Statistical Analysis

All data were expressed as the mean and the standard deviation. Statistical analysis of differences was performed with use of the student t test. The level of significance was set at $p < 0.05$. Statistical analysis of differences of the length of

the reconstructed ligament that had its origin at the isometric point was performed with use of repeated-measures analysis of variance.

Results

Normal Length Changes of the Ligaments

Lateral Ulnar Collateral Ligament

The three-dimensional animations of the elbow joint showed that all three paths of the lateral ulnar collateral ligament gradually detoured to the lateral side during flexion because of the osseous protrusion of the lateral condyle (Fig. 3). The lateral ulnar collateral ligament was not constrained by the

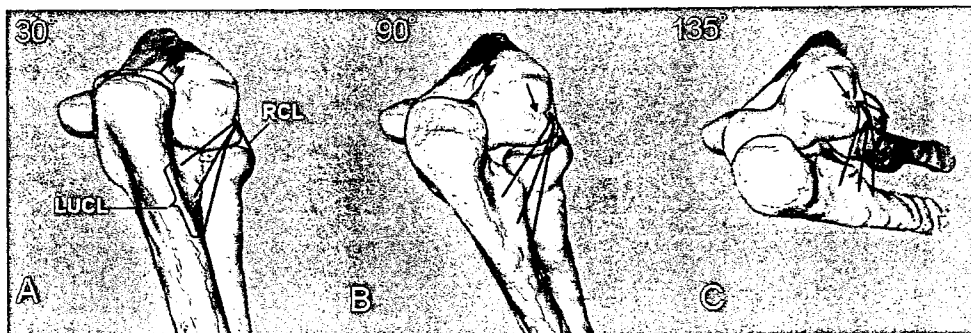


Fig. 3

The ligament paths of the lateral ulnar collateral ligament (LUCL) and the radial collateral ligament (RCL) at 30° (A), 90° (B), and 135° (C) of flexion in a representative case. The right elbows are seen from a posterolateral view. Note that the lateral ulnar collateral ligament paths detour around the osseous protrusion of the lateral condyle at 90° and 135° flexion (arrows).

TABLE I (Continued)

Length Change of Reconstructed LUCL from 0° to 135° of Flexion (mm)									Average Length of Reconstructed LUCL at 2 mm Proximal to Center and 0 mm Anterior to Center (mm)
Humeral Origin†									
Anterior to Center (mm)	0	0	2	2	2	4	4	4	
Proximal to Center (mm)	2	4	0	2	4	0	2	4	
	-0.1	-0.2	-0.6	-4.2	-3.0	-3.8	-4.0	-5.1	43.1 ± 0.9
	-0.1	-1.8	-1.6	-3.0	-4.3	-5.3	-6.3	-7.3	38.6 ± 0.6
	-1.0	-2.3	-2.2	-3.9	-5.2	-5.1	-6.5	-8.3	40.6 ± 0.7
	-1.2	-1.8	-1.6	-2.7	-3.4	-4.2	-3.9	-6.7	38.6 ± 0.7
	-0.3	-2.5	-1.4	-3.1	-4.8	-4.7	-6.1	-7.6	36.1 ± 0.4
	-1.1	-0.3	-1.6	-2.0	-2.9	-4.7	-5.3	-5.7	38.8 ± 0.6
	-1.4	-1.3	-0.1	-0.9	-1.9	-4.0	-3.5	-4.8	39.9 ± 0.8
	-0.7	-1.4	-1.3	-2.8	-3.6	-4.5	-5.1	-6.5	
	0.6	1.0	0.8	1.1	1.2	0.6	1.3	1.3	

lateral condyle in full extension. However, at about 30° of flexion, the lateral ulnar collateral ligament made contact with the posterolateral edge of the lateral condyle at approximately one-fifth of the ligament length on the proximal side of the ligament; then, with further elbow flexion, the lateral ulnar collateral ligament started to detour to the lateral side (Fig. 4) (see Appendix). These findings were true for all seven volunteers in the study.

The three-dimensional distances between the center of the capitellum and the three insertions of the lateral ulnar collateral ligament were found to increase during elbow flexion. The average length change for the three lateral ulnar collateral ligament paths was 2.6 ± 0.9 mm. The increase in length when the insertion point was 5, 15, and 25 mm distal to the radial head was 3.5 ± 0.7 mm, 2.5 ± 0.5 mm, and 1.9 ± 0.5 mm, respectively (Table I).

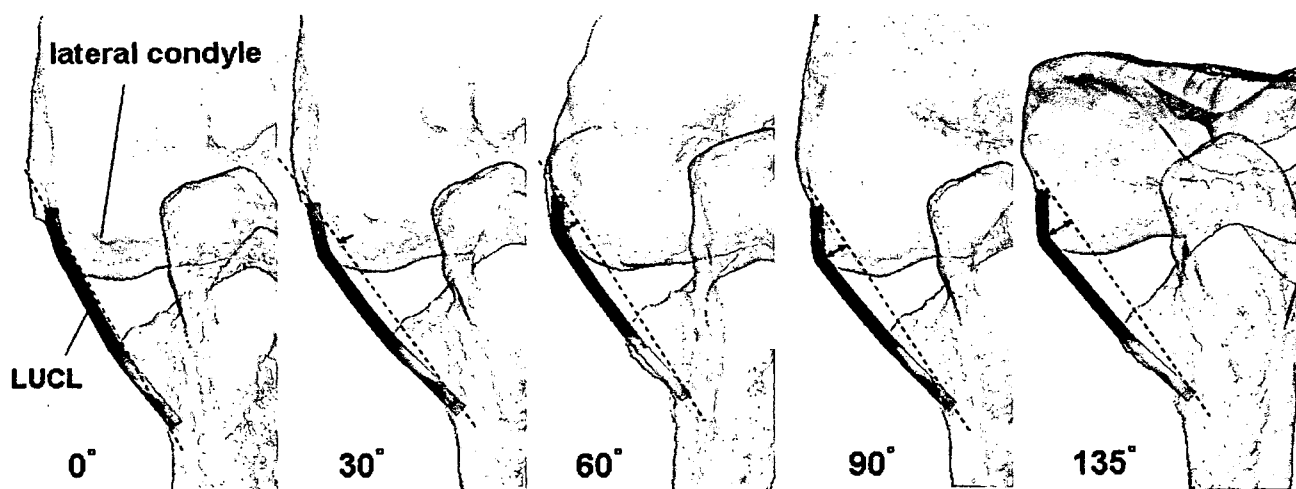


Fig. 4
The typical paths of the lateral ulnar collateral ligament (LUCL) of the right elbow from an anterior view during flexion in a representative case. The ulna is fixed, and the humerus moves; the radius is not seen in these views. Note that, with the elbow flexing, the lateral ulnar collateral ligament paths are gradually detoured by the lateral condyle.

Radial Collateral Ligament

The three-dimensional animations of the elbow joint demonstrated that the radial collateral ligament was not constrained by the lateral condyle in any position of elbow flexion in any of the seven volunteers (Fig. 3). The three-dimensional distance between the center of the capitellum and the radial head increased by 0.3 ± 1.0 mm during flexion (Table I). The increase in the length of the radial collateral ligament was significantly less than that of the lateral ulnar collateral ligament when the insertion point was 5 mm ($p < 0.00005$), 15 mm ($p < 0.0005$), and 25 mm ($p < 0.005$).

Length Changes of the Reconstructed Lateral Ulnar Collateral Ligament

The length changes of the ligament paths for the eight different humeral origins were calculated (Table I). The most isometric point of the reconstructed lateral ulnar collateral ligament was found to be located 2 mm proximal (and 0 mm anterior) to the center of the capitellum; at this point, the average length change was -0.7 ± 0.6 mm. The second most isometric point was 2 mm anterior (and 0 mm proximal) to the center of the capitellum, with an average length change of -1.3 ± 0.8 mm, and the third most isometric point was 4 mm proximal (and 0 mm anterior) to the center of the capitellum, with an average length change of -1.4 ± 1.0 mm. The length of the reconstructed ligament that had its origin at a point 2 mm proximal (and 0 mm anterior) to the capitellar center was constant and did not change significantly through the six elbow flexion positions (Table I).

Discussion

In the present study, the three-dimensional distance of the lateral ulnar collateral ligament, which was defined as the distance between the center of the capitellum and the supinator crest of the ulna, was found to increase gradually during elbow flexion, whereas that of the radial collateral ligament changed little. The path of the lateral ulnar collateral ligament detoured around the osseous protrusion of the lateral condyle with elbow flexion, whereas the radial collateral ligament was not constrained by the lateral condyle in any position of elbow flexion. These results suggest that the lateral ulnar collateral ligament is not isometric; that is, it is loose in elbow extension and becomes tight with elbow flexion. Our data also suggest that the radial collateral ligament is essentially isometric and can provide stability throughout the range of elbow flexion. Therefore, in terms of elbow stability, we consider the radial collateral ligament to be more important than the lateral ulnar collateral ligament.

Some authors have attributed the cause of posterolateral rotatory instability to the lateral ulnar collateral ligament^{11,12}. However, some recent anatomical studies have indicated that more than half of the cadavers lacked an obvious and thick lateral ulnar collateral ligament¹⁸. Also, some biomechanical studies have shown that the lateral ulnar collateral ligament can be transected without inducing posterolateral rotatory in-


stability of the elbow¹³. The results of the present in vivo study are in agreement with those findings, which cast doubt on the theory that the lateral ulnar collateral ligament is crucial to elbow stability. We speculate that the lateral ulnar collateral ligament may be a secondary stabilizer of the lateral collateral ligamentous complex.

Nevertheless, the lateral ulnar collateral ligament reconstruction procedure that is performed for the treatment of posterolateral rotatory instability has been reported to be a successful and effective procedure¹³⁻¹⁵. At the time of the ligament reconstruction, knowledge of the isometric point of the lateral ulnar collateral ligament is important because stability throughout the range of elbow motion cannot be achieved without the reconstructed ligaments being fixed to the isometric point. The isometric point of the lateral ulnar collateral ligament has been thought to be identical to the axis of rotation and to be located at the center of the capitellum, and, therefore, clinically, a drill-hole has been placed at that location^{14,15}. However, on several occasions, we have found during surgery that the reconstructed ligament became loose upon elbow extension whereas it was tight with elbow flexion. Therefore, we have often added a side-to-side suture for the reconstructed lateral ulnar collateral ligament to the remnant of the radial collateral ligament and the annular ligament. Doing so bends the path of the lateral ulnar collateral ligament slightly anteriorly, which approximates its path to being almost the same as that of the normal course of the radial collateral ligament and the annular ligament. This bending of the reconstructed ligament anteriorly may be one reason why this type of lateral ulnar collateral ligament reconstruction has been reported to be successful and effective.

In the present study, we found that the isometric point of the reconstructed lateral ulnar collateral ligament was not located at the center of the capitellum but was located 2 mm proximal to it. Therefore, to obtain more stability with use of a single graft during reconstruction of the lateral ulnar collateral ligament, we recommend that a proximal drill hole be located 2 mm proximal to the center of the capitellum. Even though the resultant ligament path is not the anatomic path, empirically it should result in stability throughout the range of elbow flexion.

The present study had some limitations. The origin and insertion of the ligaments were determined only on the basis of general anatomic information; individual variances in ligamentous and skeletal anatomy were not taken into account. Our findings are only theoretical and have not been tested surgically. However, the paths that we generated provide useful visual information about the ligaments and help to identify potential joint mobility constraints imposed by the ligaments.

Appendix

 A video demonstrating the course of the simulated lateral ulnar collateral ligament with elbow motion is available with the electronic versions of this article, on our

web site at jbjs.org (go to the article citation and click on "Supplementary Material") and on our quarterly CD-ROM (call our subscription department, at 781-449-9780, to order the CD-ROM). ■

NOTE: The authors thank Takehiro Arimura, RT, of the Department of Radiology, and Ryoji Nakao, MEng, of the Department of Orthopaedics, Osaka University Graduate School of Medicine, for their assistance during parts of the experimental procedures.

Hisao Moritomo, MD, PhD
Tsuyoshi Murase, MD, PhD
Sayuri Arimitsu, MD
Kunihiro Oka, MD
Hideki Yoshikawa, MD, PhD
Kazuomi Sugamoto, MD, PhD
Department of Orthopaedic Surgery, Osaka University, 2-2 Yamadaoka,
Suita-shi, Osaka 565-0871, Japan

References

- Olsen BS, Sojbjerg JO, Dalstra M, Sneppen O. Kinematics of the lateral ligamentous constraints of the elbow joint. *J Shoulder Elbow Surg.* 1996;5:333-41.
- Olsen BS, Sojbjerg JO, Nielsen KK, Vaesel MT, Dalstra M, Sneppen O. Posterolateral elbow joint instability: the basic kinematics. *J Shoulder Elbow Surg.* 1998;7:19-29.
- Dunning CE, Zarzour ZD, Patterson SD, Johnson JA, King GJ. Ligamentous stabilizers against posterolateral rotatory instability of the elbow. *J Bone Joint Surg Am.* 2001;83:1823-8.
- Morrey BF, An KN. Functional anatomy of the ligaments of the elbow. *Clin Orthop Relat Res.* 1985;201:84-90.
- London JT. Kinematics of the elbow. *J Bone Joint Surg Am.* 1981;63:529-35.
- Deland JT, Garg A, Walker PS. Biomechanical basis for elbow hinge-distractor design. *Clin Orthop Relat Res.* 1987;215:303-12.
- Goto A, Moritomo H, Murase T, Oka K, Sugamoto K, Arimura T, Nakajima Y, Yamazaki T, Sato Y, Tamura S, Yoshikawa H, Ochi T. In vivo elbow biomechanical analysis during flexion: three-dimensional motion analysis using magnetic resonance imaging. *J Shoulder Elbow Surg.* 2004;13:441-7.
- Crisco JJ, Coburn JC, Moore DC, Akelman E, Weiss AP, Wolfe SW. In vivo radiocarpal kinematics and the dart thrower's motion. *J Bone Joint Surg Am.* 2005;87:2729-40.
- Moritomo H, Murase T, Goto A, Oka K, Sugamoto K, Yoshikawa H. In vivo three-dimensional kinematics of the midcarpal joint of the wrist. *J Bone Joint Surg Am.* 2006;88:611-21.
- Marai GE, Laidlaw DH, Demiralp Ç, Andrews S, Grimm CM, Crisco JJ. Estimating joint contact areas and ligament lengths from bone kinematics and surfaces. *IEEE Trans Biomed Eng.* 2004;51:790-9.
- O'Driscoll SW. Classification and evaluation of recurrent instability of the elbow. *Clin Orthop Relat Res.* 2000;370:34-43.
- O'Driscoll SW, Bell DF, Morrey BF. Posterolateral rotatory instability of the elbow. *J Bone Joint Surg Am.* 1991;73:440-6.
- Nestor BJ, O'Driscoll SW, Morrey BF. Ligamentous reconstruction for posterolateral rotatory instability of the elbow. *J Bone Joint Surg Am.* 1992;74:1235-41.
- Olsen BS, Sojbjerg JO. The treatment of recurrent posterolateral instability of the elbow. *J Bone Joint Surg Br.* 2003;85:342-6.
- Lee BR, Teo LH. Surgical reconstruction for posterolateral rotatory instability of the elbow. *J Shoulder Elbow Surg.* 2003;12:476-9.
- Lorenson WE, Cline HE. Marching cubes: a high resolution 3D surface construction algorithm. *ACM SIGGRAPH Comput Graph.* 1987;21:163-9.
- Cohen MS, Hastings H 2nd. Rotatory instability of the elbow. The anatomy and role of the lateral stabilizers. *J Bone Joint Surg Am.* 1997;79:225-33.
- Takahashi K, Minami A, Kato H, Kasajima T, Hirachi K. Anatomical study of lateral ligament complex of the elbow. *J Jpn Elbow Soc.* 1997;4:15-6.

IL-1 β promotes neurite outgrowth by deactivating RhoA via p38 MAPK pathway

Ko Temporin ^a, Hiroyuki Tanaka ^{a,b,*}, Yusuke Kuroda ^a, Kiyoshi Okada ^a, Koji Yachi ^a, Hisao Moritomo ^a, Tsuyoshi Murase ^a, Hideki Yoshikawa ^a

^a Department of Orthopaedics, Osaka University Graduate School of Medicine, Suita, Osaka 565-0871, Japan

^b Medical Center for Translational Research, Osaka University Hospital, Suita, Osaka 565-0871, Japan

Received 15 October 2007

Available online 8 November 2007

Abstract

Expression of the pro-inflammatory cytokine interleukin-1 beta (IL-1 β) is increased following the nervous system injury. Generally IL-1 β induces inflammation, leading to neural degeneration, while several neuropoietic effects have also been reported. Although neurite outgrowth is an important step in nerve regeneration, whether IL-1 β takes advantages on it is unclear. Now we examine how it affects neurite outgrowth. Following sciatic nerve injury, expression of IL-1 β is increased in Schwann cells around the site of injury, peaking 1 day after injury. In dorsal root ganglion (DRG) neurons and cerebellar granule neurons (CGNs), neurite outgrowth is inhibited by the addition of myelin-associated glycoprotein (MAG), activating RhoA. IL-1 β overcomes MAG-induced neurite outgrowth inhibition, by deactivating RhoA. Intracellular signaling experiments reveal that p38 MAPK, and not nuclear factor-kappa B (NF- κ B), mediated this effect. These findings suggest that IL-1 β may contribute to nerve regeneration by promoting neurite outgrowth following nerve injury. © 2007 Elsevier Inc. All rights reserved.

Keywords: Interleukin-1 beta; Neurite outgrowth; RhoA; Dorsal root ganglion neuron; Cerebellar granule neuron; Nerve regeneration; p38 MAPK; Nuclear factor-kappa B

Interleukin-1 beta (IL-1 β) is a pro-inflammatory cytokine, the expression of which is increased in the nervous system following injury [1,2]. IL-1 β induces the production of toxic mediators, such as inflammatory molecules and cytokines, and promotes inflammation and cell death, and as a result it leads to neurodegeneration [3]. On the other hand, several beneficial effects of IL-1 β on the nervous system have also been reported, such as promotion of Schwann cell proliferation [4], promotion of neuron survival [5,6], oligodendrocyte remyelination [7], and synthesis of nerve growth factor by sciatic non-neuronal cells [8]. Thus whether IL-1 β promotes or delays nerve regeneration remains to be clearly determined.

Neurite outgrowth is an important process in nerve regeneration. Various effects of inflammatory cytokines on neurite outgrowth have been reported; tumor necrosis factor- α inhibits neurite outgrowth in hippocampal neurons [9], while interleukin-6 overcomes neurite outgrowth inhibition by myelin-associated glycoprotein (MAG) in dorsal root ganglion (DRG) neurons [10]. Only one report is available on the effects of IL-1 β on neurite outgrowth, and indicates that IL-1 β promotes neurite outgrowth in DRG explant culture but not in dissociated single DRG neuron culture, and that glial cells mediate these opposing effects [11].

Neurite outgrowth is regulated by the small GTPase RhoA, activation of which leads to neurite outgrowth inhibition [12]. Following nerve injury, myelin-derived proteins such as MAG, Nogo-A, and oligodendrocyte myelin glycoprotein activate RhoA in neurons and inhibit neurite outgrowth [13]. The effects of IL-1 β on neurite outgrowth

* Corresponding author. Address: Department of Orthopaedics, Osaka University Graduate School of Medicine, Suita, Osaka 565-0871, Japan. Fax: +81 6 6879 3559.

E-mail address: tanahiro-osk@umin.ac.jp (H. Tanaka).

with regard to RhoA or myelin-derived inhibitors of neurite outgrowth have not been reported.

In this study, we demonstrate a novel function of IL-1 β , i.e. overcoming RhoA activation and neurite outgrowth inhibition by MAG in DRG neuron and cerebellar granule neuron (CGN) culture. Our findings thus suggest that the pro-inflammatory cytokine IL-1 β may aid regeneration of the injured nervous system.

Materials and methods

Cell culture. DRG neurons were cultured as described previously [14]. DRGs from Wistar rats at postnatal day 9 or 10 were dissociated by incubation with 0.25% trypsin, 0.1% collagenase, and 200 U/ml DNase I. The enzymatic reaction was blocked by adding DMEM containing 10% FBS, and after trituration and centrifugation, cells were resuspended in Sato medium and plated in poly-L-lysine-coated 4-well chambers.

For CGN culture, cerebellum from Wistar rats at postnatal day 7–10 was dissociated by incubation with 0.25% trypsin and 200 U/ml DNase I. The enzymatic reaction was blocked by adding DMEM containing 10% FBS, and after trituration and centrifugation, cells were resuspended in Sato medium. After additional centrifugation, cells were resuspended in Sato medium and plated in poly-L-lysine-coated culture dishes or 4-well chambers.

Sciatic nerve crush injury. Female Wistar rats (180–220 g) were anesthetized by intraperitoneal injection of sodium pentobarbital (50 mg/kg). The left sciatic nerves were exposed at mid-thigh level, and then fine forceps, the tip of which had been cooled in liquid N₂ before use, were used to crush the nerve for 15 s. The site of crush injury was marked by 10–0 nylon, and muscle and skin were then sutured.

Histological analysis. The rats were anesthetized by sodium pentobarbital, and transcardially perfused with PBS, followed by 4% paraformaldehyde. The sciatic nerve was then removed, embedded in paraffin, sectioned axially at 5 μ m, and mounted on glass slides.

Immunostaining. The 4-well chambers or glass slides were fixed in 4% paraformaldehyde for 30 min, blocked for 1 h, and incubated overnight at 4 °C with primary antibody, followed by incubation for 1 h at room temperature with fluorescein-conjugated secondary antibody (Molecular Probes). The primary antibodies used were anti-IL-1 β goat polyclonal antibody (R&D Systems), anti-S100 rabbit polyclonal antibody (DAKO), anti-neurofilament (NF) 200 rabbit antiserum (Sigma–Aldrich), and anti-neural class III β -tubulin (TuJ1) mouse monoclonal antibody (Covance).

Neurite outgrowth assay. Neurons were cultured with 50 ng/ml IL-1 β (Peprotech), 25 μ g/ml MAG (R&D Systems), 10 μ M Y27632 (Calbiochem), 20 μ M SN50 (Calbiochem), 20 μ M SN50M (Calbiochem), or 1 μ M SB203580 (Calbiochem) for 72 h and then immunostained with anti-TuJ1 antibody. The longest neurites of TuJ1-positive neurons were measured for axonal length as described previously [15] using an image analyzer (Lumina Vision, Mitani Co., Japan). Results were obtained from at least 60 neurons in each group.

Western blotting. Nerve tissues or culture cells were homogenized with Kaplan buffer (50 mM Tris, pH7.4, 150 mM NaCl, 10% glycerol, 1% NP40, and protease inhibitor cocktail) and clarified by centrifugation. They were separated on SDS-PAGE and transferred to polyvinylidene difluoride membranes. After blocking, the membranes were incubated with anti-IL-1 β goat polyclonal antibody or anti- β -actin mouse monoclonal antibody (Sigma–Aldrich), followed by horseradish peroxidase-conjugated secondary antibodies (GE Healthcare) and ECL reagents (GE Healthcare).

Rho assay. Rho assay was performed as described previously [16]. Briefly, CGNs were lysed in lysis buffer, and the cell lysates were clarified by centrifugation and incubated for 45 min with Rho Assay Reagent (Upstate) to selectively bind activated RhoA for the pull-down assay. The beads were washed with washing buffer. Whole-cell lysates were directly immunoblotted to determine the total amount of RhoA. RhoA was

detected by Western blotting using anti-RhoA mouse monoclonal antibody (Santa Cruz Biotechnology).

ELISA. Uninjured or injured sciatic nerves were cut into 7 mm pieces. To obtain conditioned media, nerves were incubated in DMEM/F-12 containing 10% FBS (200 μ l per nerve) for 5 h, and conditioned media were clarified by centrifugation. To obtain nerve extract, nerves were homogenized in Kaplan buffer and clarified by centrifugation. Each sample of conditioned medium and nerve extract was produced with three distinct nerves. Sandwich ELISA was then performed to quantify IL-1 β according to the manufacturer's instructions (Quantikine; R&D Systems).

Results and discussion

IL-1 β is expressed in Schwann cells following sciatic nerve injury

Since expression of IL-1 β is known to be increased following nerve injury [1,2], we examined its pattern of expression in a sciatic nerve crush injury model of rat. The sciatic nerves were injured in rats and removed 1, 3 or 7 days after injury. Immunohistochemistry revealed that following sciatic nerve injury, expression of IL-1 β was increased 1 day after injury, and that this increase in expression persisted until 7 days (Fig. 1A). Expression of IL-1 β is found in Schwann cells and macrophages *in vitro* [2], though a clear observation of its cellular localization using methods such as immunohistochemistry and *in situ* hybridization has not been reported *in vivo*. To confirm the pattern of cellular localization of IL-1 β , we used anti-NF antiserum for axons and anti-S100 antibody for Schwann cells in immunohistochemical study. At 1 day after injury, IL-1 β was expressed in Schwann cells and not in axons (Fig. 1B). Since macrophages, a possible source of IL-1 β , migrate into peripheral nerve at 3 days after crush injury [17], when the peak of expression of IL-1 β has already passed, Schwann cells are considered to be the principal source of IL-1 β following peripheral nerve injury. To investigate the site of expression, crushed sciatic nerve was divided into four segments around the site of injury (Fig. 1C) and the expression of IL-1 β was estimated in each segment. Since IL-1 β is synthesized as a 31 kDa precursor (pro-IL-1 β), and cleaved to a 17 kDa mature form by caspase-1 before being released extracellularly [18], the expression of pro-IL-1 β was also examined. Expression of pro-IL-1 β (31 kDa) was observed in proximal and distal segments at 1 day by Western blotting and persisted until 7 days after injury, though to only a slight extent (Fig. 1D). Since mature IL-1 β could not be detected by Western blotting, expression of soluble IL-1 β was examined by ELISA as described previously [2]. Since the expression of pro-IL-1 β was not changed in the most proximal segment (P2) during the period of observation, the other three segments (P1, D1, and D2) were examined in detail at 1, 3, and 7 days after injury. In conditioned medium, in which injured sciatic nerve segment had been soaked and which contained mature IL-1 β , expression of IL-1 β was increased at 1 day and persisted until 3 days after injury (Fig. 1E). Using sciatic nerve extract, which

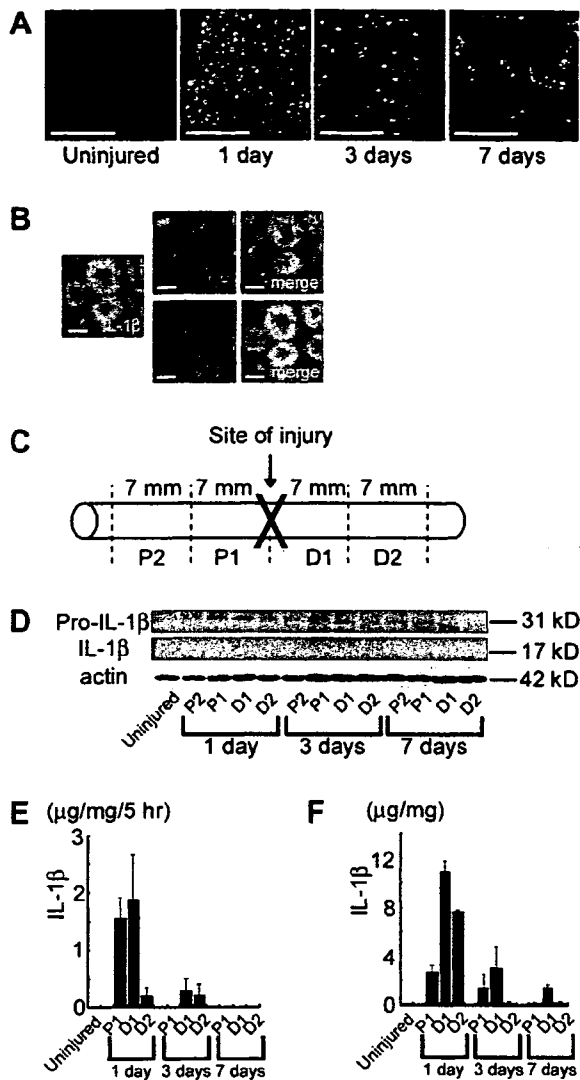


Fig. 1. Expression of IL-1 β following sciatic nerve injury. (A) Fluorescence micrographs of sciatic nerves of uninjured rats and 2 mm proximal to the site of injury at 1, 3, and 7 days after crush injury using anti-IL-1 β antibody. Bar: 100 μ m. (B) Fluorescence micrographs of consecutive sections 2 mm proximal to the site of injury at 1 day after injury using anti-IL-1 β antibody and anti-NF antisera or anti-S100 antibody. Bar: 5 μ m. (C) Sciatic nerves were transected in 7 mm lengths in the segments proximal and distal to the site of injury at 1, 3, or 7 days after injury, and were used in Western blotting and ELISA. Proximal segments (P1 and P2) are on the left and distal segments (D1 and D2) on the right. (D) Using the lysates from transected sciatic nerves, expressions of pro-IL-1 β and IL-1 β were examined by Western blotting. (E and F) Expression of IL-1 β was examined by ELISA using conditioned medium (E) and transected nerve extract (F). Error bars indicate means \pm SEM. Results are representative of three independent experiments.

contained both pro- and mature IL-1 β , expression of IL-1 β also peaked at 1 day, and persisted until 7 days after injury (Fig. 1F), consistent with the results of Western blotting (Fig. 1D). These findings suggest that after sciatic nerve injury, IL-1 β is expressed in Schwann cells both proximal and distal to the site of injury.

IL-1 β overcomes MAG-induced neurite outgrowth inhibition by deactivating RhoA

We next examined the effects of IL-1 β on neurite outgrowth. Horie et al. have reported that IL-1 β promotes neurite outgrowth in DRG explant culture, but not in dissociated single DRG neuron culture, and that this effect appears to be mediated by neurotrophic factors from non-neuronal cells [11]. In their study, neurite outgrowth is estimated in only two groups, a control and an IL-1 β group, in dissociated single DRG neuron culture. After central and peripheral nerve injury, myelin-derived proteins, such as Nogo-A and MAG, inhibit neurite outgrowth by activating RhoA [13,19], and it is important that the effects of these inhibitory molecules be overcome in nerve regeneration. We therefore cultured primary DRG neurons in the presence or absence of MAG and IL-1 β , and estimated neurite outgrowth using immunofluorescence. Fluorescence micrographs of DRG neurons (Fig. 2A) showed that MAG inhibited neurite outgrowth and that addition of IL-1 β inhibited this effect of MAG on neurite outgrowth. As measured by axonal length in DRG neurons, MAG inhibited neurite outgrowth ($138.6 \pm 7.8 \mu$ m) compared with the control ($176.3 \pm 7.1 \mu$ m), while IL-1 β with MAG enhanced it ($180.4 \pm 11.0 \mu$ m) compared with MAG. Addition of IL-1 β alone did not change axonal length ($176.5 \pm 7.5 \mu$ m). IL-1 β had the same effect on axonal length in CGNs as in DRG neurons (Fig. 2C). MAG reduced axonal length ($244.1 \pm 11.3 \mu$ m) compared with control ($293.5 \pm 13.1 \mu$ m), and IL-1 β in addition to MAG results in the same axonal length ($295.0 \pm 10.4 \mu$ m) as in the control. These findings suggest that IL-1 β overcame neurite outgrowth inhibition induced by MAG.

RhoA is a small GTPase of the Rho family and functions by switching between inactive GDP-bound and active GTP-bound states. The Rho family plays essential roles in cellular morphology, such as the actin cytoskeleton in stress fibers, lamellipodia, and filopodia [20]. In neurons, RhoA, acting through downstream Rho kinase, is responsible for various morphological changes, such as growth cone collapse, retraction of neurites, and axonal repulsion [21]. Following peripheral and central nerve injury, released MAG and other factors bind to Nogo receptor, yielding activation of RhoA, which brings about neurite outgrowth inhibition [22]. We therefore examined RhoA activity by Rho pull-down assay using CGNs (Fig. 2D and E). Because RhoA activation by MAG peaks at 15 min [23], cells were cultured with MAG or IL-1 β for 15 min before being lysed. MAG increased RhoA activity (2.2-fold compared with control), and the addition of IL-1 β attenuated it (1.0-fold compared with control) to control level. On the other hand, no change in RhoA activity was observed with IL-1 β alone (1.0-fold compared with control). These findings indicate that IL-1 β inhibited the activation of RhoA promoted by MAG.

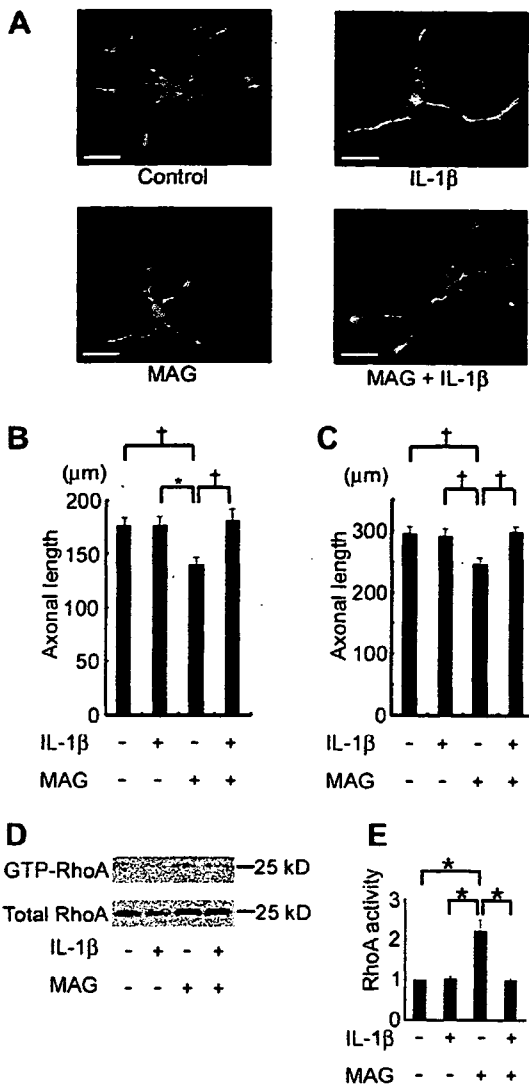


Fig. 2. Effects of IL-1β on neurite outgrowth. (A and B) Fluorescence micrographs using anti-TuJ1 antibody (A) and axonal length (B) of DRG neurons. Bar: 100 μm. (C) Axonal length of CGNs. (D and E) Rho pull-down assay (D) and quantification of results (E) using CGNs. Relative activities were quantified compared to the control group. Significance of differences was determined by *t*-test. **p* < 0.05 and †*p* < 0.01. Error bars indicate means ± SEM. Results are representative of three independent experiments.

p38 MAPK mediates the inhibition by IL-1β RhoA activity

DRG neurons and CGNs express the specific receptor of IL-1β, type I interleukin-1 receptor (data not shown), and signal is transmitted intracellularly through it. The principal intracellular pathways of IL-1β are known to proceed through nuclear factor-kappa B (NF-κB) and MAPKs, p38 MAPK, and c-Jun N-terminal kinase [24]. We therefore examined the intracellular signaling pathway of IL-1β in neurite outgrowth assay using two specific inhibitors, SN50 for the NF-κB pathway and SB203580 for the p38 MAPK pathway.

In the NF-κB pathway, NF-κB is necessary for CGN survival [25]. In our investigation addition of SN50 for

15 min did not have effect on neuronal viability, while addition for 3 days induced CGN apoptosis (data not shown). Thus we performed neurite outgrowth assay using DRG neurons alone. Neurite outgrowth assay of DRG neurons revealed that SN50 reduced axonal length (129.0 ± 4.5 μm) compared with its control peptide SN50M (168.7 ± 15.5 μm) (Fig. 3A). This effect appeared to be due to activation of RhoA, since the addition of SN50 increased RhoA activity to 2.0-fold compared with that of SN50M in CGN neurons (Fig. 3B and C). This was demonstrated by the finding that addition of Y27632, an inhibitor of Rho kinase, increased axonal length (158.1 ± 9.7 μm) compared with SN50 alone (Fig. 3A). Addition of Y27632 alone is reported not to enhance axonal outgrowth in CGNs [23], and thus this result suggests that Rho kinase is the downstream of NF-κB. Moreover, since IL-1β in addition to SN50 enhanced axonal outgrowth (149.6 ± 6.5 μm) (Fig. 3A) and decreased RhoA activity (0.7-fold compared with SN50M) relative to SN50 (Fig. 3B and C). These findings suggest that IL-1β overcame neurite outgrowth inhibition by deactivating RhoA, and not via the NF-κB pathway. Since NF-κB also enhances neurite outgrowth in the developing nervous system [26] and is required for CGN survival [25], it is essential for the nervous system development. NF-κB does not mediate the effect of IL-1β.

On the other hand, with regard to the p38 MAPK pathway, neurite outgrowth assay revealed that SB203580 reduced axonal length (157.4 ± 12.2 μm in DRG neurons, 247.8 ± 15.6 μm in CGNs) compared with that in the DMSO group (215.3 ± 12.6 mm in DRG neurons, 323.3 ± 18.6 in CGNs) (Fig. 4A and B). The activation of RhoA appeared to be responsible for this, since the addi-

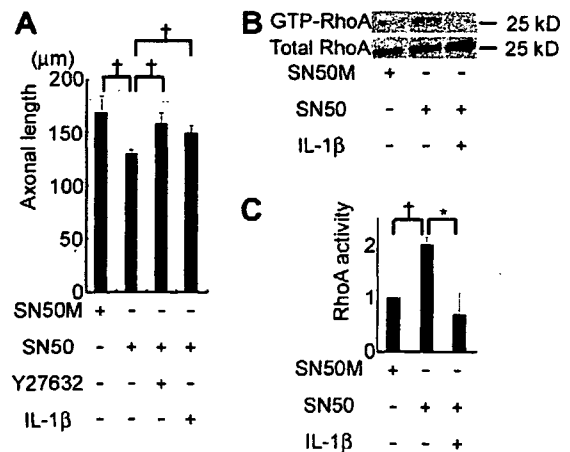


Fig. 3. IL-1β overcame neurite outgrowth inhibition, though not via NF-κB pathway. (A) Axonal lengths were measured in DRG neuron culture using SN50M, SN50, Y27632, or IL-1β. (B and C) Rho pull-down assay was performed using CGNs (B) and intensities were measured (C). CGNs were cultured with SN50M, SN50, or IL-1β for 15 min before lysed. Relative activities were quantified compared to the SN50M group. Error bars indicate means ± SEM. **p* < 0.05 and †*p* < 0.01. Results are representative of three independent experiments.